International Journal of
Physics and Mathematics

E-ISSN: 2664-8644
P-ISSN: 2664-8636
IJPM 2025; 7(2): 109-117
© 2025 IJPM
www.physicsjournal.net
Received: 08-06-2025
Accepted: 11-07-2025

Poonam Agarwal
Guru Nanak Khalsa College of
Arts, Science and Commerce,
Matunga, Mumbai, Maharashtra,
India

Corresponding Author:
Poonam Agarwal
Guru Nanak Khalsa College of
Arts, Science and Commerce,
Matunga, Mumbai, Maharashtra,
India

Finite difference method for electrostatic potential and field simulation

Stanislav Ordin

DOI: https://www.doi.org/10.33545/26648636.2025.v7.i2b.133

Abstract
This paper presents a numerical solution to the two-dimensional Poisson equation using the finite difference method over a square domain. The partial differential equation is discretized using finite difference approximations subject to Dirichlet boundary conditions. The resulting system of linear equations is solved iteratively to solve potential distributions for various charge configurations. Potential distribution and electric field lines of point charge, dipole and quadrupole are simulated in the study. The numerical implementation is performed in Python, an open-source programming language.

Keywords: Python, poisson equation, partial differential equation, finite difference method, electric potential and field

Introduction

The Poisson equation is a fundamental partial differential equation. These equations appear in various field of physics such as electrostatics, fluid dynamics, head conduction through solids etc. [1, 2, 3]. Analytical solutions are only feasible for simple geometries and boundary conditions. For more complex domains or when mixed boundary conditions are involved, numerical methods are typically used. Modern programming tools such as Python are well-suited for implementing numerical techniques like finite difference method (FDM). Python's extensive libraries for numerical computation (such as NumPy) and data visualization library (Matplotlib) make it an effective platform for modelling and solving partial differential equations.

Poisson equation can be derived from Gauss's law [2, 3, 4]. Gauss's law is written as

$$\vec{\nabla} \cdot \vec{E} = \frac{\rho}{\varepsilon_0} \qquad (1)$$

where $\vec{E}$ is the electrostatic field, ρ (x, y, z) represents the charge density, ε_0 is the permittivity of the free space. Electric field can be written as negative gradient of potential (V) as

$$\vec{E} = \vec{\nabla} V \qquad (2)$$

Substituting Eq. (2) in Eq. (1), we get

$$\nabla^2 V = -\frac{\rho}{\varepsilon_0} \qquad (3)$$

Eq. (3) is known as Poisson's equation. In cartesian coordinates, it can be written as

$$\frac{\partial^2 V}{\partial x^2} + \frac{\partial^2 V}{\partial y^2} + \frac{\partial^2 V}{\partial z^2} = -\frac{\rho}{\varepsilon_0} \qquad (4)$$

In two-dimension, Poisson's equation is represented as

$$\frac{\partial^2 V}{\partial x^2}+\frac{\partial^2 V}{\partial y^2}=-\frac{\rho}{\varepsilon_0} \quad (5)$$

Eq. (5) relates the electric potential at a point in xy plane to the charge density at that point. In charge free region ($\rho = 0$), eq. (5) reduces to Laplace's equation.

$$\frac{\partial^2 V}{\partial x^2}+\frac{\partial^2 V}{\partial y^2}=0 \quad (6)$$

Eq. (5) and Eq. (6) are widely used to solve the boundary value problems. These problems involve finding the electric field and potential within a domain when certain boundary conditions are specified [1, 2, 3, 4]. These conditions define how potential and electric field behave at boundary. When potential is specified at all the boundaries, the solution of the Poisson equation is unique in the domain. This type of boundary condition is known as Dirichlet boundary condition. In Neumann boundary condition, the normal component of electric field (derivative of potential) is specified at the boundary.

This paper deals with numerical solution of two-dimensional Poisson equation for computing and visualizing potential and electric field near point charges. In the present study, potential and field near an elementary charge distribution such as point charge, dipole and quadrupole have been investigated. These configurations are modelled numerically using finite difference method (FDM) to solve Poisson equation in two dimensions on square domain [5, 6, 7]. FDM is implemented in python. The resulting potential distribution and electric field patterns are visualized and analysed to validate the numerical technique.

Finite Difference Method

In this method, computational domain is discretized in a uniform two-dimensional grid with a fixed spacing along x and y directions. Each grid point is represented as (x_i, y_i). The potential $V(x_i, y_i)$ and charge density $\rho(x_i, y_i)$) at a point (x_i, y_i) in the domain is written as $V(i,j)$ and $\rho(i,j)$ respectively. If Δx and Δy represent the grid spacing along x and y directions then,

$$x_i = i \cdot \Delta x \text{ for } i = 0,1,2,\ldots\ldots N_x$$

$$y_j = j \cdot \Delta y \text{ for } j = 0,1,2,\ldots\ldots N_y$$

N_x and N_y are the total number of grid points along x and y directions respectively. Using central difference scheme, partial derivatives can be written as

$$\frac{\partial^2 V}{\partial x^2}=\frac{V(i+1,j)-2V(i,j)+V(i-1,j)}{(\Delta x)^2}$$

$$\frac{\partial^2 V}{\partial y^2}=\frac{V(i,j+1)-2V(i,j)+V(i,j-1)}{(\Delta y)^2}$$

Since derivatives are expressed in terms of the finite differences in the values of V at the grid points, this is called a finite-difference method [5, 6, 7]. Eq. (5) can be written in terms of finite differences as

$$\frac{V(i+1,j)-2V(i,j)+V(i-1,j)}{(\Delta x)^2}+\frac{V(i,j+1)-2V(i,j)+V(i,j-1)}{(\Delta y)^2}=-\frac{\rho(i,j)}{\varepsilon_0} \quad (7)$$

For every point (i,j) on the mesh. Setting $\Delta x = \Delta y = h$ for the square grid, Eq. (7) can be written as

$$V(i,j)=\frac{1}{4}\left[V(i+1,j)+V(i-1,j)+V(i,j+1)+V(i,j-1)+h^2\frac{\rho(i,j)}{\varepsilon_0}\right] \quad (8)$$

Eq. (8) holds for all interior points on the grid. It shows that the value of potential at each node (i,j) is the average of the potential at the four neighboring points and contribution from local charge density. Thus, second order partial differential equation is transformed into a set of simultaneous equations one for each interior grid point. The solution set of entire system of equations gives us the solution $V(i,j)$ at each grid point. The continuous solution of Eq. (4) is approximated by the solution $V(i,j)$ on the grid point. The accuracy of this method is therefore connected to the ability of a finite grid to approximate a continuous system, and errors may be reduced by increasing the number of grid points [8].

An iterative method is used to solve these simultaneous equations. An iterative method begins with an initial estimate, which is then used to obtain the second approximation. It is refined step by step to produce a sequence of improved approximations. Each new estimate is derived from the previous one, and the process continues until the desired level of accuracy or tolerance is achieved. Among the widely used iterative techniques are the Jacobi method, the Gauss-Seidel method and the Successive Over-Relaxation (SOR) method [5, 6, 7]. The present study involves the SOR method for the computation.

Successive Over-Relaxation (SOR) method

The basic structure of the Finite Difference Method (FDM) often requires a very fine grid to achieve accurate results. This fine discretization increases the number of nodes significantly, which in turn demands more computational storage and a larger number of iterations to reach convergence. To accelerate the convergence process, the Successive Over-Relaxation (SOR) method is used [5, 6, 7, 8]. This method improves the rate of convergence by introducing a relaxation factor (ω), into the iterative update process. The relaxation formula for the new values $V^{k+1}(i,j)$ in terms of old values $V^k(i,j)$ can be written as

$$V^{k+1}(i,j) = V^k(i,j) + \frac{\omega}{4}R^k(i,j)$$

Where $R(i,j)$ is the residual at node (i,j) and is defined as

$$R(i,j) = V(i+1,j) + V(i-1,j) + V(i,j+1) + V(i,j-1) + h^2\frac{\rho(i,j)}{\varepsilon_0}$$

The value of the residual at kth iteration is denoted as $R^k(i,j)$. It may be regarded as the correction which may be added to $V(i,j)$ to get the values close to the correct value. As convergence to the correct value is approached, $R^k(i,j)$ tends to zero. Using the SOR method, the potential at grid point after $(k+1)$th iteration can be written as

$$V^{k+1}(i,j) = (1-\omega)V^k(i,j) + \frac{\omega}{4}\left[V^k(i+1,j) + V^k(i-1,j) + V^k(i,j-1) + V^k(i,j+1) + h^2\frac{\rho(i,j)}{\varepsilon_0}\right] \quad (9)$$

In SOR method, the relaxation parameter (ω) influences the rate of convergence. When $\omega = 1$ the method is equivalent to the Gauss-Seidel algorithm, and values $0 < \omega < 1$ corresponds to under relaxation. When 1 < ω < 2 corresponds to "overrelaxation" and an appropriate choice of ω can lead to faster convergence of the algorithm. When ω > 2, SOR method fails to converge.

The electric field $\vec{E}$ is the **negative gradient** of the potential (V). It can be evaluated at all interior points using central difference scheme.

$$E_x(i,j) = -\frac{V(i+1,j) - V(i-1,j)}{2h}$$

$$E_y(i,j) = -\frac{V(i,j+1) - V(i,j-1)}{2h}$$

On the boundaries one sided forward/backward difference scheme can be used.

Algorithm

Algorithm of the computation consists of the following steps:

- Decide the computation domain. Mesh size h is chosen. The domain is dicretized into a uniform grid of size $(N+1) \times (N+1)$ including the points on the boundary.
- The simulation is started with initial guess for the potential which is represented by a matrix $V(i, j)$. Boundary values are assigned with fixed potential on the edges of the domain.
- A charge density matrix $\rho(i,j)$ is initialized with all zero elements to represent distribution of charge on the domain is created. The desired charge configuration is then assigned by setting the appropriate nonzero vales at the specific grid points.
- Sweep all interior grid points and determine $V(i,j)$ using Eq. 9 for SOR method for iteration.
- This procedure is iterated a number of times such that the potential at each node does not change much in the next iteration.
- The iterative process is terminated when the maximum change in potential between successive iterations falls below a predefined threshold ($\max_{i,j}|V_{new} - V_{old}| < \varepsilon$), where ε is tolerance. For the present work tolerance is set at 10^{-6}.
- Algorithm is implemented in Python. NumPy and Matplotlib libraries were used for the computation and visualization of the results.

Results and Discussion

Poisson's equation is solved numerically using FDM for various charge distributions over a square domain of size 1x1 m^2 in xy plane. Dirichlet boundary conditions were applied in the problem where the electric potential was set to zero along all four boundaries. Boundary condition is given by

$$V(0,y) = V(1,y) = V(x,0) = V(x,1) = 0$$

To obtain the solution, the SOR method was implemented to accelerate the convergence of the iteration process. Program was run for various values of relaxation factor ω in the range of 1.5 to 1.9 to optimize the performance.

Simulations were carried out for various charge configuration including single point charge (monopole), dipole and quadrupole. For each charge configuration, equipotential lines, surface plot of potential distribution and electric field were drawn to visualize the results. Equipotential lines are the curves on which potential is constant. Surface plots are the three-dimensional representations of the potential. Electric fields are perpendicular to the equipotential lines. Strong electric fields correspond to packed or dense equipotential lines. Electric field vectors show the direction and magnitude of the electric field across the domain.

A. Point charge

For this simulation, a single point charge is placed at the centre of the square domain. The charge is modelled with a normalized source strength, $\frac{\rho}{\varepsilon_0} = 100$ V/m^2 located at x = 0.5 m, y = 0.5 m. The four edges of the region are grounded. Since the domain is discrete, we can consider that the node at the centre of the domain describes an area around the point, and the charge density only exists in this small (but finite) area [8]. Solution was obtained for $\omega = 1.9$ and system converged after 192 iterations. Figure 1 shows the contour plot showing equipotential lines of the point charge.

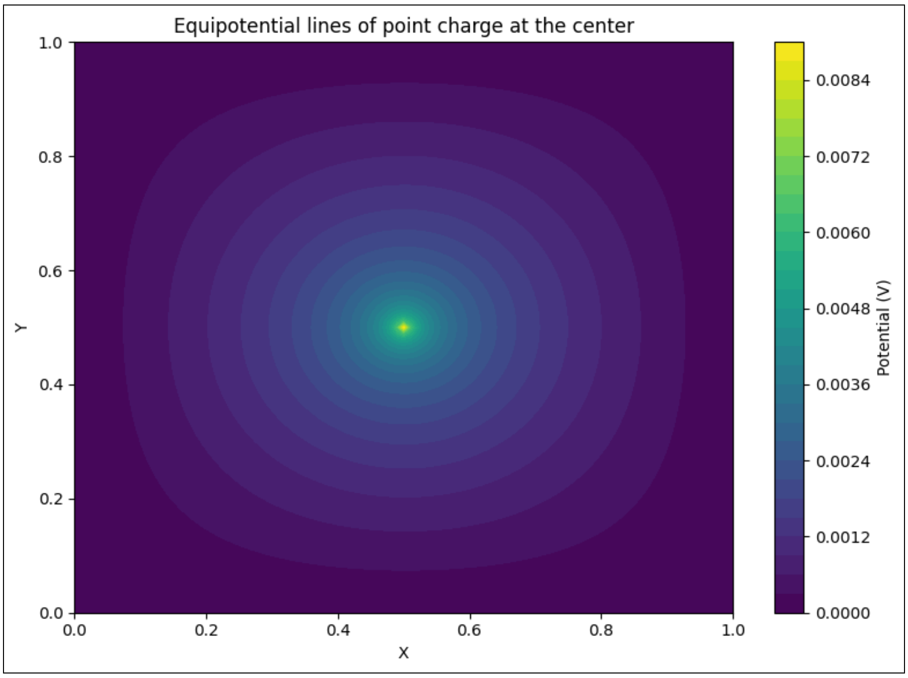

Fig 1: Equipotential lines of a point charge at the centre $\frac{\rho}{\varepsilon_0} = 100$ V/m^2

Figure 2 represents zoomed-in contour plot of the potential distribution (from 0.4 m to 0.6 m) which focuses on the central region of the domain where charge is placed.

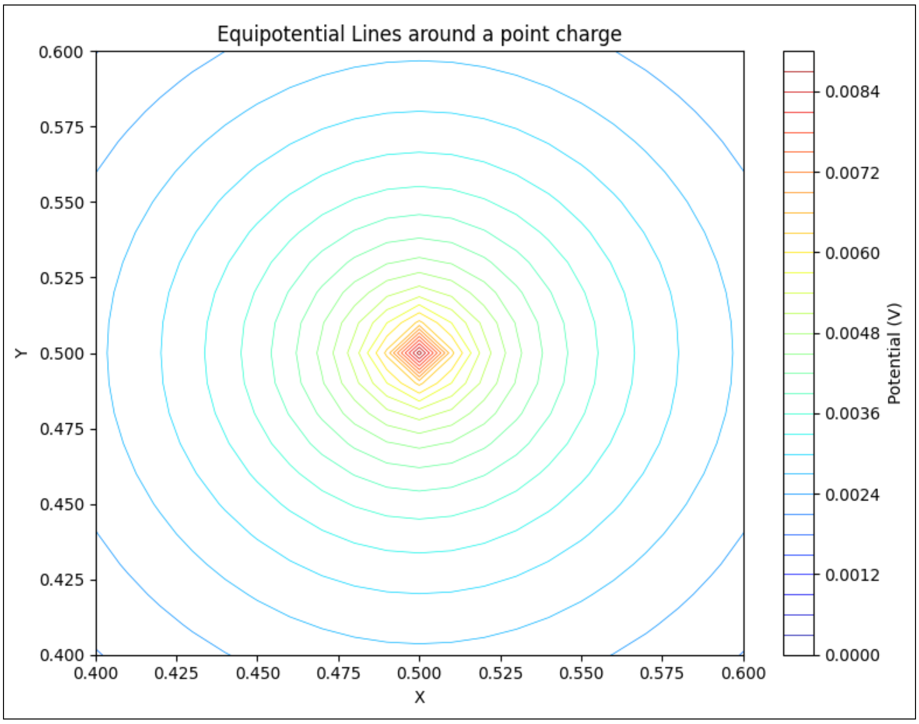

Fig 2: Zoomed-in contour plot of the central region showing the equipotential lines near the point charge

Figure1 show that the potential contours form circular equipotential lines in a plane around the charge consisting with the radial symmetry as expected for the point charge. However figure 2 shows that the equipotential curves are not perfectly circular near the charge. This deviation occurs because simulation models a point charge placed at the centre of a grounded region not a free charge. Because of square symmetry of the domain, it acquires a slightly square in shape at the edges also. Because of the finite size of the grid, this effect is more pronounced near the charge [7]. Figure 3 illustrates the electric field lines of the point charge.

The electric field points radially outwards. The electric field strength is highest near the charge and decrease with the distance from the centre. As observed from contour plot (Figure 1), equipotential lines dense near the charge, therefore, potential gradient in that region is high indicating strong field near the charge. It weakens as it approaches the grounded boundaries.

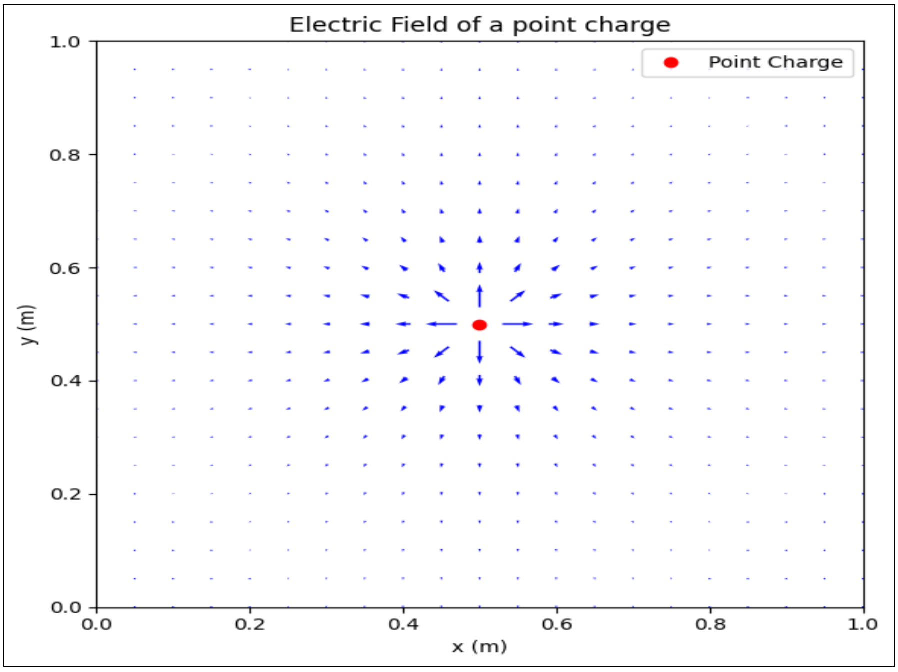

Fig 3: Electric field lines of a point charge.

B. Point charge near one edge of the domain

For this simulation, a charge of strength, $\frac{\rho}{\varepsilon_0} = 100$ V/m^2 is considered at the centre ($x = 0.25\ m$, $y = 0.5\ m$) of the square domain. The four edges of the region are grounded. Figure 4 shows the potential distribution around the point in xy plane.

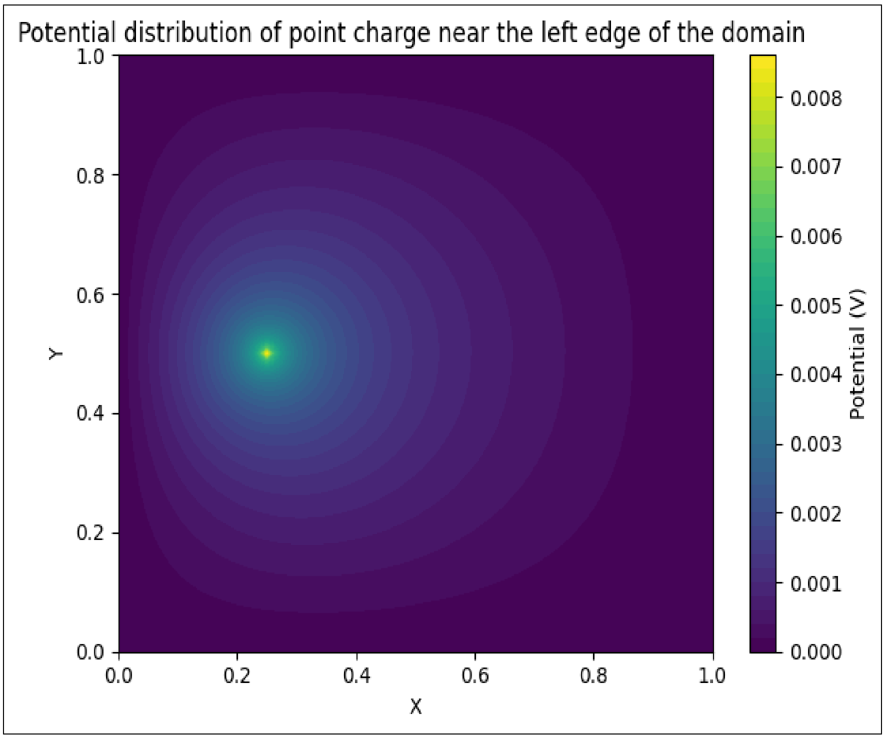

Fig 4: Equipotential lines around a point charge $\left(\frac{\rho}{\varepsilon_0} = 100\ V/m^2\right)$2 at the near one edge of the domain (x=0.25 m, y=0.5 m). All the four sides are kept at zero potential.

Potential distribution is not symmetric due to non-symmetric placement of the charge related to the square boundaries.

Figure 5 Shows the electric field lines near the charge.

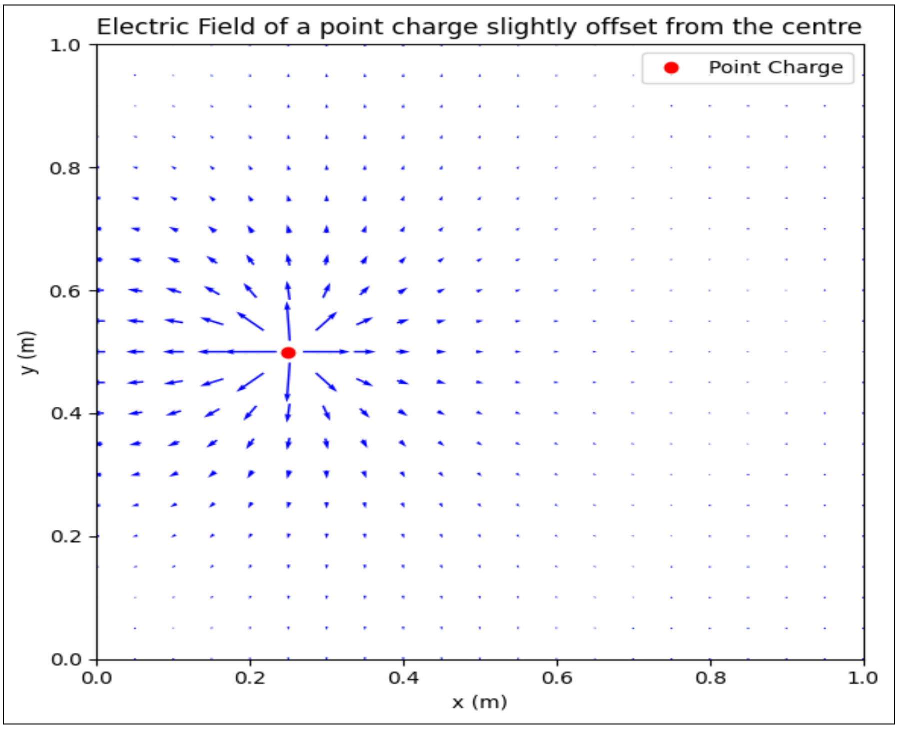

Fig 5: Electric field lines of a point charge at x = 0.25m, y = 0.5m

The electric field is antisymmetric around the charge. Equipotential lines are more packed on the side which is closer to the grounded boundary indicating strong electric field in that region. Field lines originate from positive charge and terminate perpendicularly on the grounded edges.

C. Dipole

For dipole, two opposite charges are placed symmetrically about the centre of the domain. For this configuration, a charge of strength, $\frac{\rho}{\varepsilon_0} = 100$ V/m^2 is placed at x = 0.4 m, y = 0.5 m and a negative charge $\frac{\rho}{\varepsilon_0} = -100$ V/m^2 is placed at x = 0.6 m, y = 0.5 m of the square domain. Therefore, dipole is aligned along the x-axis. Computation was completed in 112 iterations with $\omega = 1.9$. Figure 6 and Figure 7 show the equipotential lines and potential distribution of the dipole.

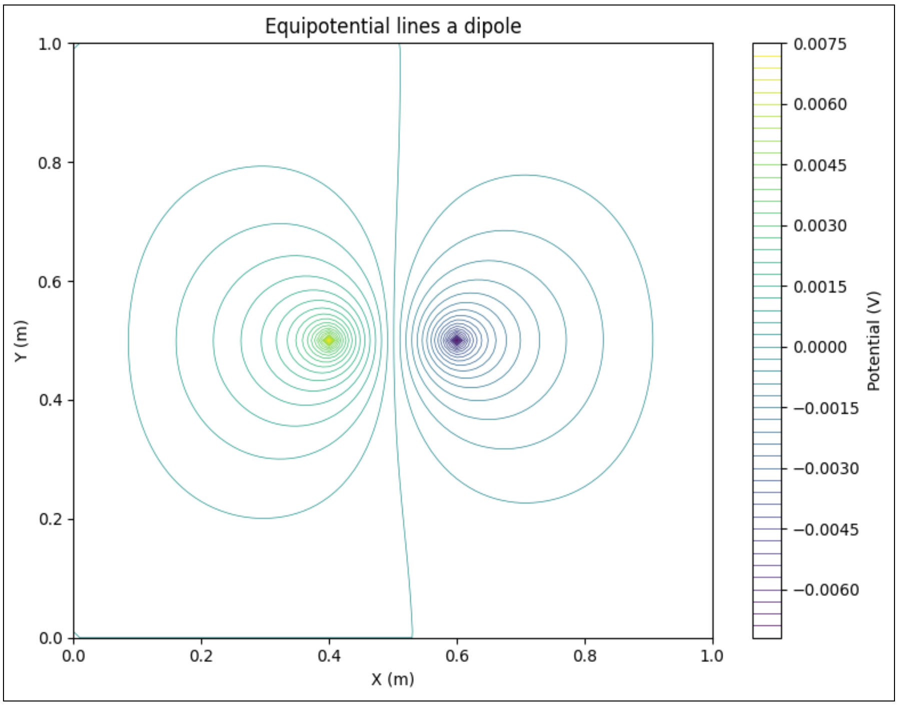

Fig 6: Equipotential lines of a dipole symmetrically placed about the centre along x-axis

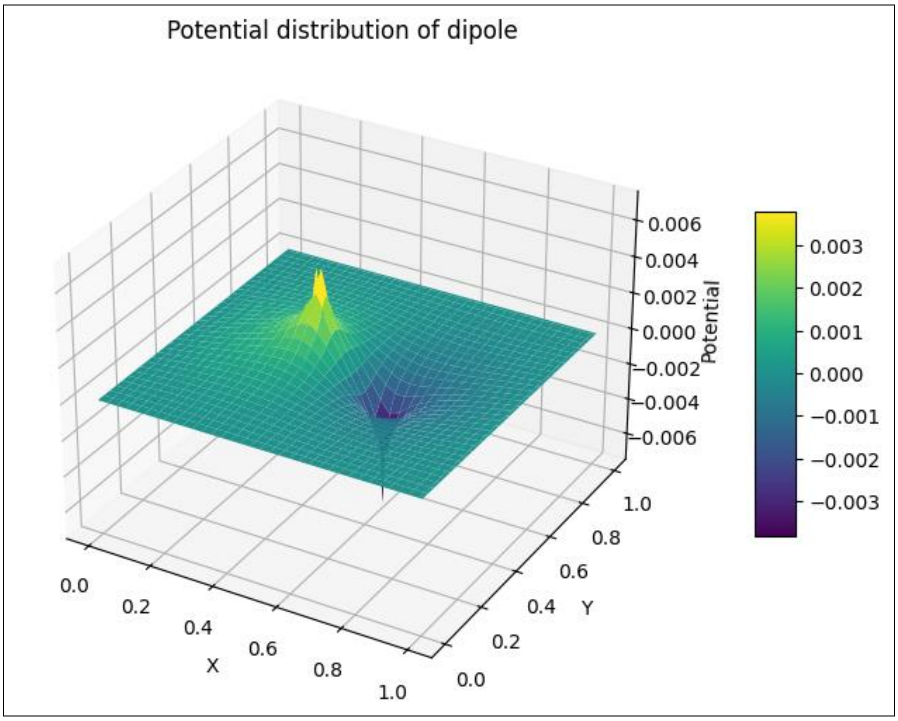

Fig 7: Surface plot of potential distribution of a dipole

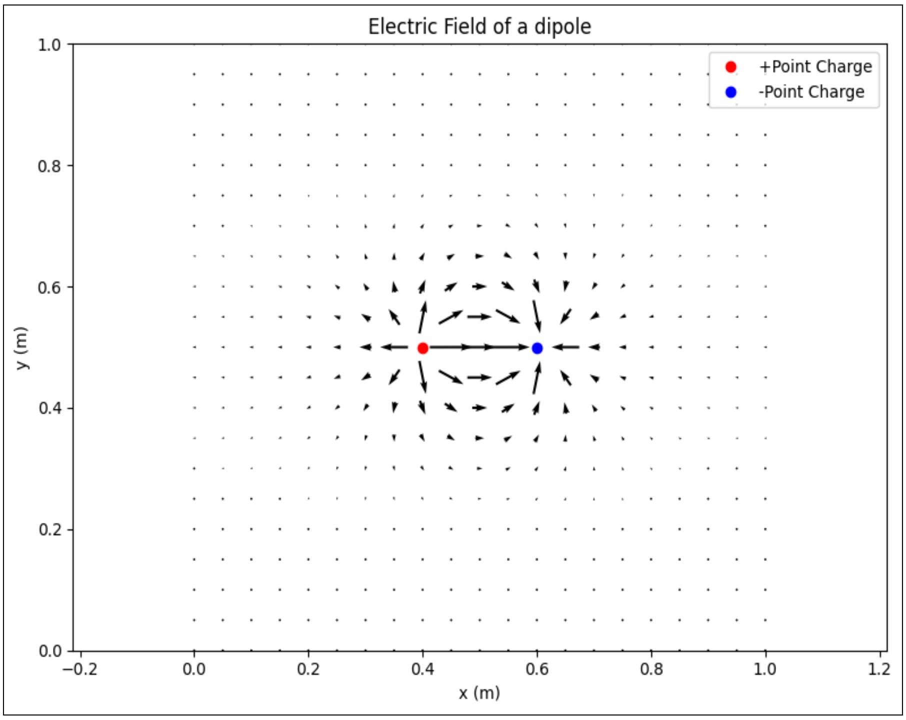

Fig 8: Electric field vectors of a dipole

The equipotential lines are symmetric and show two lobes for positive and negative potential around positive and negative charge respectively. Electric field lines originate from positive charge and terminate on negative charge. In surface plot (Figure 7) a sharp peak shows the location of positive charge and a negative peak appears at the location of negative charge. Potential changes rapidly in the near the two charges indicating presence of strong electric field in that region. Potential slowly decreases to zero near the boundaries.

D. Quadrupole

For quadrupole, two oppositely oriented dipoles are placed symmetrically about the centre of the domain. For this configuration, two positive charges of normalized magnitude $\frac{\rho}{\varepsilon_0} = 100$ V/m^2 are placed at x = 0.4 m, y = 0.6 m and x = 0.6 m, y = 0.4 m. Two negative charges of same magnitude are placed at x = 0.4 m, y = 0.4 m and x = 0.6 m, y = 0.6 m on the square domain with grounded boundaries.108 iterations are required to reach the convergence with $\omega = 1.9$. Figure 9 and Figure 10 show the equipotential lines and potential distribution of the quadrupole.

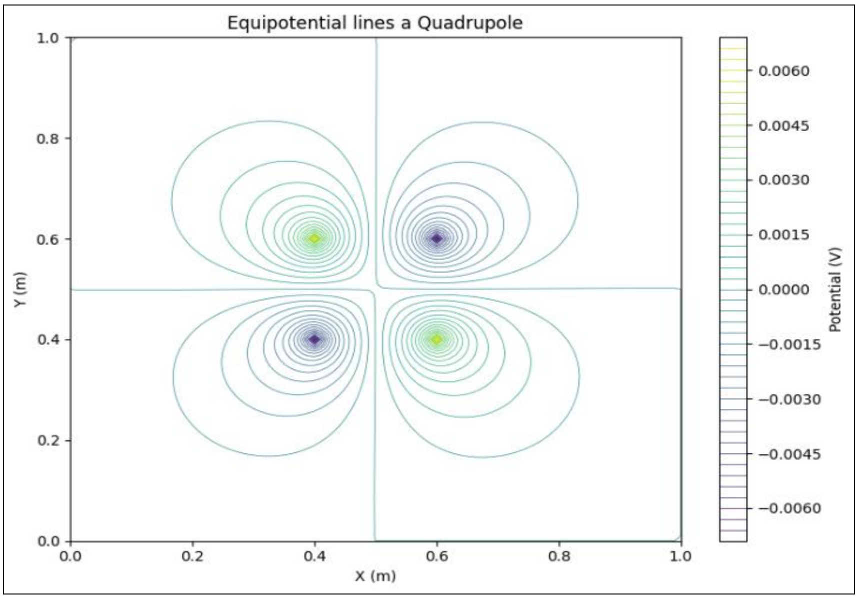

Fig 9: Equipotential lines of a quadrupole symmetrically placed about the centre.

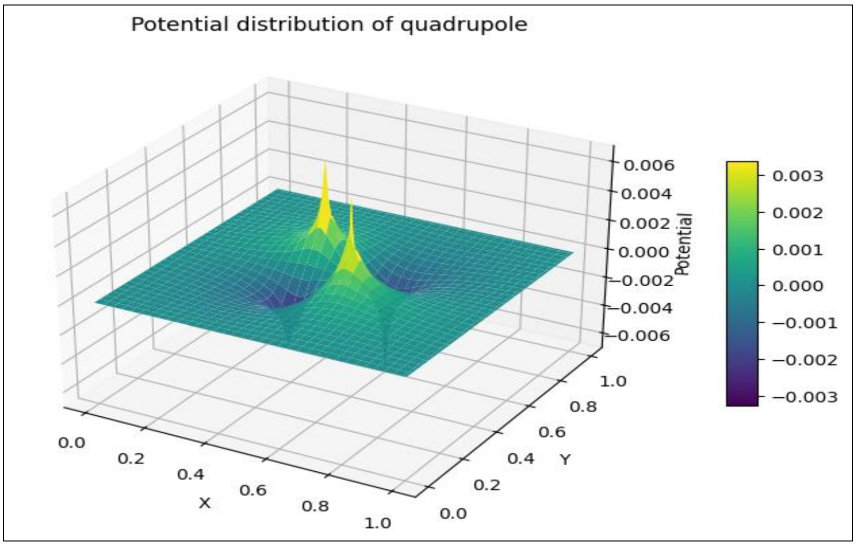

Fig 10: Surface plot of potential distribution of a quadrupole

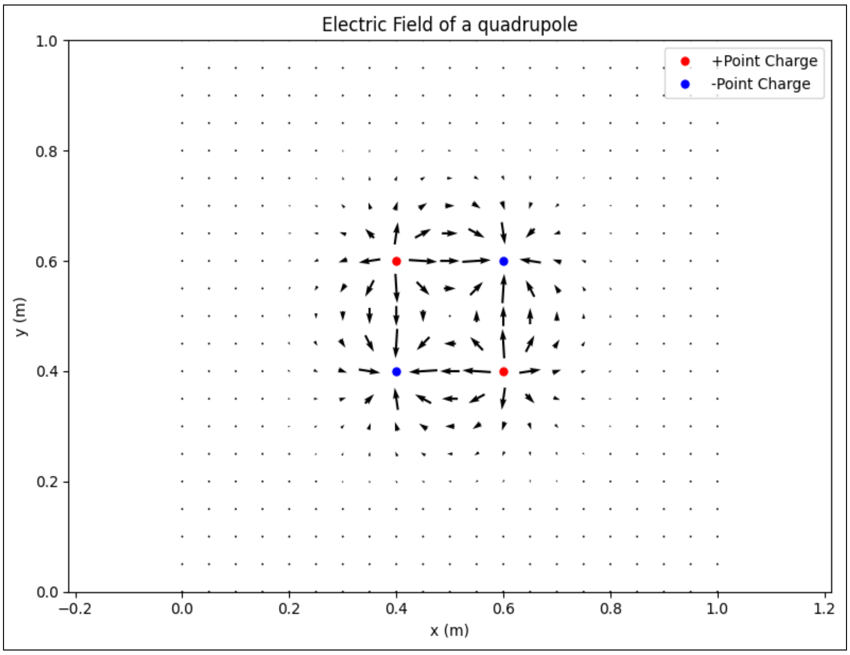

Fig 11: Electric field vectors of a quadrupole

Equipotential lines show positive and negative lobes placed alternatively about the centre. Surface plot shows two positive peaks where the positive charges are located and two negative peaks where the negative charges are located. At the geometrical centre, the potential is nearly zero because of the symmetry of the charge distribution. Surface plot shows the saddle point at the centre. Around each charge, surface plot shows a sharp rise or fall in the potential indicating presence of strong electric field. Figure 11 shows the electric field pattern near the quadrupole.

Conclusion

This work presented a numerical simulation of various electrostatic charge configurations within a square domain with Dirichlet boundary condition using finite difference method. The system was iterated using successive over relaxation technique to speed up the convergence. Three charge distribution are considered for the study, a single point charge, a dipole and a quadrupole. In each case potential distribution and electric field were computed and visualized. The numerical simulation successfully reproduces the qualitative features of potential distribution and electric field near each charge configurations. The finite grid size and point charge approximations distort equipotential lines near the charge.

References

1. Boas ML. *Mathematical methods in the physical sciences*. New York: Wiley; 1966.
2. Griffiths DJ. *Introduction to electrodynamics*. New Delhi: PHI; 2002.
3. Purcell EM. *Electricity and magnetism*. New York: McGraw-Hill; 1985.
4. Sadiku MNO. *Elements of electromagnetics*. New York: Oxford University Press; 2001.
5. Landau RH, Páez MMJ, Bordeianu CC. *Computational physics: Problem solving with computers*. Weinheim: Wiley-VCH; 2007.
6. Sadiku MNO. *Numerical techniques in electromagnetics*. 2nd ed. Boca Raton: CRC Press; 2000.
7. Giordano NJ, Nakanishi H. *Computational physics*. 2nd Ed. Upper Saddle River (NJ): Pearson Prentice Hall; 2006.
8. Nagel JR. Numerical solutions to Poisson equations using the finite-difference method. *IEEE Antennas Propag Mag*. 2014;56(4):209-24.
9. Newman MEJ. *Computational physics*. Seattle (WA): Create Space Independent Publishing Platform; 2012.